BENCHMARKING OF WIND FARM SCALE WAKE MODELS IN THE EERA - DTOC PROJECT

P.-E. Réthoré[1], K.S. Hansen[1], R.J. Barthelmie[2], S.C. Pryor[2], G. Sieros[5], J. Prospathopoulos[5], J.M.L.M. Palma[4], V.C. Gomes[4], G. Schepers[3], P. Stuart[6], T. Young[6], J.S. Rodrigo[7], G.C. Larsen[1], T.J. Larsen[1], S. Ott[1], O. Rathmann[1], A. Peña[1], M. Gaumond[1] and C. B. Hasager[1]

[1]DTU, Wind Energy, Denmark, pire@dtu.dk
[2]Indiana University, Department of Geological Sciences, USA
[3]ECN, The Netherland, [4]University of Porto, Portugal
[5]CRES, Greece, [6]RES, United Kingdom, [7]CENER, Spain

ABSTRACT

Designing offshore wind farms next to existing or planned wind farm clusters has recently become a common practice in the North Sea. These types of projects face unprecedented challenges in term of wind energy siting. The currently ongoing European project FP7 EERA - DTOC (Design Tool for Offshore wind farm Clusters) is aiming at providing a new type of model work-flow to address this issue. The wake modeling part of the EERA - DTOC project is to improve the fundamental understanding of wind turbine wakes and modeling. One of these challenges is to create a new kind of wake modeling work-flow to combine wind farm (micro) and cluster (meso) scale wake models. For this purpose, a benchmark campaign is organized on the existing wind farm wake models available within the project, in order to identify which model would be the most appropriate for this coupling. A number of standardized wake cases for large offshore wind farms will be analyzed, which provide a reasonable range of conditions likely to be experienced in offshore wind farms. The systematic evaluation is based upon high - quality input data that is selected in the sister project IEA - Task 31 “WakeBench”.

INTRODUCTION

With the large offshore wind farms becoming common practice in Northern Europe, the need for reliable wind farm wake models has never been as critical as today. There exists many different

types of wind farm wake models that have been developed during the last three decades, some more complex than others. The wind industry is now to routinely calculating wind farms annual energy production (AEP) using more and more complex wind farm wake models. For instance, running non-linear Reynolds Averaged Navier-Stokes Computational Fluid Dynamics (CFD) actuator disc model has become practical for most medium size companies. In parallel, the amount data and understanding of the wind farm power production has increased significantly during the last 5 years.

The EERA-DTOC project (European Energy Research Alliance - Design Tool for Offshore wind farm Clusters) is focusing on providing a tool to design wind farm clusters, which is a combination of several offshore wind farms. An important element in this tool will be the wind farm annual production estimate, which will rely on one or several state of the art wind farm wake models. The different partners in the project have developed over the years many different offshore wind farm wake models that could be (one of) the potential candidate(s) to be implemented in the EERA-DTOC software. In order to select the right wake models a series of benchmarks are currently underway in collaboration with the IEA-Task 31 "WakeBench" project.

While previous offshore wind farm wake benchmark comparisons have been carried out during the past decade in the ENDOW project [19] and UpWind project [18], the new and refined models available for the industry combined with the better understanding and refined data of the wind farm SCADA make it relevant now to initiate a new benchmark based on the Horns Rev wind farm within the EERA-DTOC project.

This article will focus on presenting the different models with their specific sub-model assumptions, the Horns Rev wind farm, the challenges of creating a reliable reference dataset for the comparison with the wind farm wake models, the different test cases and finally a discussion of the results.

WAKE MODELS

The wind farm wake models present in the EERA-DTOC project are presented in tb. 1.

- **SCADA** is the processed wind farm data to be compared with the other wind farm wake models. Wind farm SCADA data are not usually referred in the literature as a model result. However, considering the amount of assumptions and processing methods that have to be applied in order to produce comparable results with a wind farm wake model, a processed SCADA data should in all fairness be treated as a model result. This point is further detailed in the following section.

- **Ainslie** is an eddy-viscosity wake model developed by RES-LTD [5-6] based on the original Ainslie model [8].

- **FarmFlow** is a parabolized k-ε actuator disc CFD model tailored for offshore wake simulation developed by ECN, based on the original UPM wind farm wake model from Crespo [9] combined with a vortex wake model in the close wake.

- **RANS** is an elliptic k-ε actuator disc CFD model tailored for offshore wake simulation developed by Porto University.
- **CRESflowNS** is an elliptic k-ω actuator disc CFD model tailored for offshore wake simulation developed by CRES [13-14].
- **WAsP/NOJ** is the PARK wake model of WAsP commercial software developed by DTU [10] and based on the original wake model from N.O. Jensen [11].
- **NOJ** is the original N.O Jensen model [11], using the mozaic tile methode of Rathmann [21].
- **DWM** is the Dynamic Wake Meandering model developed by DTU [16-17]. This model is the only dynamic model presented in this paper.
- **GCL** is the G.C. Larsen eddy-viscosity wake model v2009 developed by DTU [15].
- **FUGA** is a linearized actuator disc eddy-viscosity CFD model for offshore wind farm wake developed by DTU [12].

The wind farm wake models compared in this work can be categorized in different ways according to their sub-model assumptions. The sub-models considered in this analysis are:

- Inflow model: How the inflow wind speed is described
  - Log law: The log law is used to create the inflow condition, based on the sea roughness, the hub height and hub wind speed.
  - Homogeneous: The inflow is assumed to be homogeneous. Only the hub wind speed is needed.
  - TI: The turbulence intensity is needed.
  - Stability: The inflow conditions are dependent of atmospheric parameters
  - Mann: The inflow is generated through the Mann turbulence model. It can also be tuned to generate different inflow stability conditions and turbulence intensities.
- Hub wind speed model: How the wind speeds generated by the wake model are combined into an input to the wind turbine model. Here the number of points are indicated as a reference for how the turbines take into account the inflow partial wakes. The NOJ model is using a mosaic tile approach, weighting the wake wind speed with the intersectional area between the rotor and the upstream wake deficits.
- Wind turbine model: How the power and thrust are calculated:
  - HAWC2 is an aero-elastic model developed at DTU [7]
  - PTC: The Power and Thrust coefficient Curves, that takes the free-stream wind speed as a reference. Note that an additional method is required when used in combination with an elliptic CFD code in order to estimate this free-stream wind speed in wake conditions. This additional method is not considered in the present analysis.

Table 1: Sub-models assumptions

Institute	Model Name	Inflow	Hub WS	Turbine	Wake acc	Wake flow
DTU WE	SCADA	Processed wind farm SCADA measurements				
DTU WE	FUGA	Log law	7P	PTC	Linear	FUGA
DTU WE	GCL	Log law+TI	16P	PTC	Linear	GCL
DTU WE	DWM	Mann	$>$ 100P	HAWC2	Max.	DWM
DTU WE	NOJ	Homog.	Mosaic	PTC	RSS	NOJ
Indiana Uni	WAsP/NOJ	Homog.	Mosaic	PTC	RSS	NOJ+GPR
RES-LTD	Ainslie	Homog.+TI	1P	PTC	ARL	Ainslie+GPR
CRES	CRESflowNS	Log law	1P	PTC	Elliptic k-ω	
Porto Uni	RANS	Log law	1P	PTC	Elliptic k-ε	
ECN WE	FarmFlow	Stability	1P	PTC	Vortex + Parabolic k-ε	

- Wake accumulation model: How the wake contributions are accumulated
  - Linear: add the velocity deficits.
  - RSS: Root-Sum-Square (i.e. Quadratic).
  - k-ω or k-ε : The accumulation is done by solving the Reynolds Averaged Navier-Stokes equations.
  - Maximum: The maximum wake deficit is used.
  - ARL: Average RSS and Linear velocity deficits.
- Wake flow model: How the wake of one or several wind turbines is calculated. Each model has a different way to solve the momentum and mass flow conservation equation and to account for the inflow and wake generated turbulence. The CFD type models account directly for the ground plane through the Navier-Stokes equations (i.e. FUGA, RANS, CRESflowNS, FarmFlow); some use a Ground Plane Reflection (GPR) method (i.e. Ainslie, WAsP/NOJ); finally, some do not account for the ground surface (i.e. NOJ, GCL and DWM).

DATA PRESENTATION AND ANALYSIS

Horns Rev Wind Farm

The Horns Rev wind farm (HR) has a shared ownership by Vattenfall AB (60%) and DONG Energy AS (40%). It is located 14 km from the west coast of Denmark, with a water depth of 6-14 m. The wind farm has a rated capacity of 160 MW comprising 80 wind turbines, which

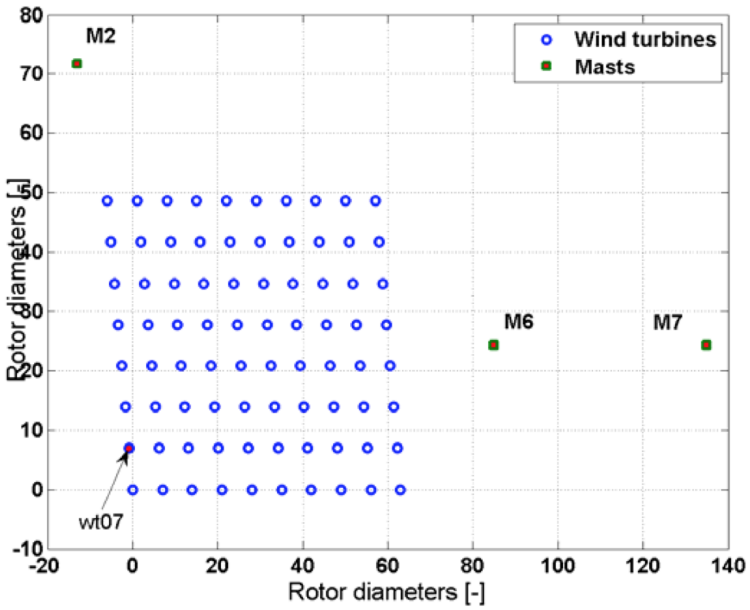

Figure 1: Horns Rev wind farm layout

are arranged in a regular array of 8 by 10 turbines, with a spacing of 560 m in both directions covering an area of 5x3.8 km2. The layout of the wind farm, fig. 1, is not completely rectangular, while the direction of the N-S columns is 353°. The wind turbines are installed with an internal spacing along the main directions of 7D. The diagonal wind turbine spacing is either 9.4 D or 10.4 D. Fig. 1 illustrates the location of the three offshore meteorological masts associated with the wind farm. Mast M2, with a height of 62m, was installed prior to the wind farm installation to document the wind conditions. Two identical masts M6 and M7 were installed as part of the Horns Rev wind farm wake measurements program with a height equal to the hub height of 70m. The wind farm comprises VESTAS V80 turbines, which are 2 MW pitch controlled, variable speed wind turbines with a diameter of 80 m and 70 m hub height. The wind farm has been in operation since 2004 and the SCADA statistics from 2005 – 2007 is available for the wake analysis [1].

The dataset for the current wake analysis was limited to three years, from 2005 to 2007, and includes the SCADA data from the 80 wind turbines and the two downstream wake masts (M6 & M7). Due to the local wind rose, the wake analysis shall be concentrated to westerly and easterly inflow sectors centered at 270° and 90° respectively. Because M6 & M7 are located inside the wind farm wake for the 270° sector, a flow reference has been establish based on wt07 (located in the most western row of the wind farm) in terms of wind speed derived from electrical power and wind direction derived from the calibrated wind turbine yaw position. For the western flow sector, the power curve of wt07 has been validated with wind speed measurements from M2, 62 m level [1]. None of the wind turbine yaw position sensors have been calibrated while these are not used in the wind turbine control, but the yaw position offset for wt07 has been calibrated

and found to be constant during the period, according to the guidelines in [2]. The estimated uncertainty of the wind direction is 5°. For the eastern flow sector, the measured wind speed and wind directions are recorded at 70 m level on either M6/M7.

Definition of power deficit

For westerly inflow, the power deficit is determined with respect to the reference wt07:

$$\text{Power Deficit} = \frac{P_{\text{wt07}} - P_{\text{wt}}}{P_{\text{wt07}}} \tag{1}$$

For easterly inflow, the power deficit is determined with respect to the reference wt95:

$$\text{Power Deficit} = \frac{P_{\text{wt95}} - P_{\text{wt}}}{P_{\text{wt95}}} \tag{2}$$

Definition of the error bars

In the plots presented in this article, the error bars on the SCADA plots are the standard uncertainty defined as

$$u = \frac{\sigma}{\sqrt{n}}, \tag{3}$$

with σ the standard deviation and n the number of 10-minute data points available for doing the averaging. Note that this value quantifies the level of confidence in the statistical representativity of the averaging, and not the amount of data spreading.

Data analysis

When looking at processed wind farm SCADA data it is quite important to keep in mind that it is the result of a number of assumptions and processing methods. For instance, fig. 2 illustrates the difference between three processing methods over the same test case: the single wake power deficit between two turbines (wt07 & wt17) in aligned in westerly inflow. All the curves are using the same data sample (2005-2009) but different wind direction sensors (the nacelle position of wind turbine wt07 (NP07) and the mast M7 wind vane), while the curve called we.512_ref is presenting the results using NP07 from another data sample, when the inflow wind was with stable stratification. The mast M7, as it can be seen in fig. 1 is located at more than 10km from the wind turbines wt07 and wt17. By using its wind vane as the sorting sensor, we make the assumption that the wind direction is the same over the distance of 10km. Because of the wind direction spatial/temporal variability, the further away the wind direction is measured, and the less likely this assumption is correct, which introduces an uncertainty in the wind direction correlated with the distance from the wind direction sensor to the wind turbine of interest. As discussed in [4], when considering ensemble average wake deficit data, an uncertainty in wind direction can have the same effect as introducing more partial wake and free wake cases into the ensemble average. So choosing M7 over a closer wind direction sensor, like NP07, gives an artificially lower wake maximum deficit.

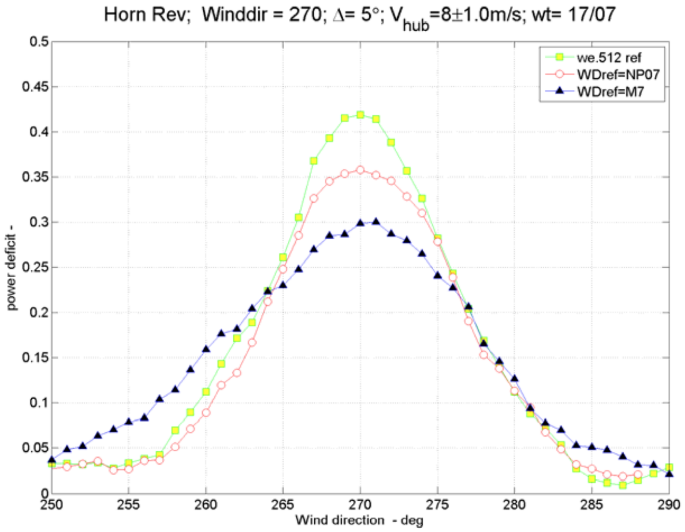

Figure 2: Wind turbine wake deficit using different inflow wind direction sensors (NP07 and M7). The single wakes are compared with a similar data presented in a reference article (we.512 ref).

The effect of wind direction spatial/temporal variability can also be seen by looking at the power deficit along different rows of wind turbines. In fig. 3, the wind direction is measured at the first turbine in the row 7. As the spatial/temporal variability is the lowest for the row 7, its power deficit is also the highest. The further away the rows are from the wind direction sensor, and the smaller the wake deficit appears to be. By taking the average of all the rows of wind turbines, the averaged line also have an artificially lower wake deficit compared with the row 7.

Even though the wind direction sensor is the closest possible, other sources of wind direction uncertainty can have a similar effect as the spatial/temporal variability over the processed wake data. Fig. 4 illustrates the probability density distribution of the power deficit along row 7 with a narrow wind direction angle bin. The results show that there is still a quite large spread of the power deficit, even though we saw previously that the results are better than in the other rows, or using another source of wind direction. Other unmeasured parameters, such as the large scale turbulence (with a time scale larger than the 10-minute averaging period) or the wind turbine yaw misalignment compared to the inflow wind direction, could introduce an uncertainty in wind direction that could cause these sort of spreading effects. Furthermore, the sub-10-minute inflow turbulence should cause a natural wake meandering of the wind turbines wake, which could also create this spreading effect. However, the wake meandering should be partially accounted for by the wake models, so it is quite difficult to dissociate the natural from the artificial spreading seen in the measurements.

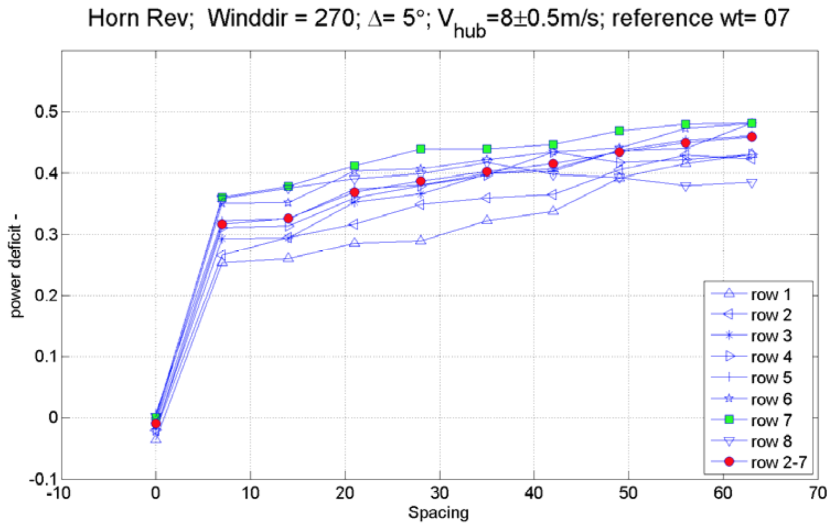

Figure 3: The power deficit along different lines of wind turbine in the westerly wind direction

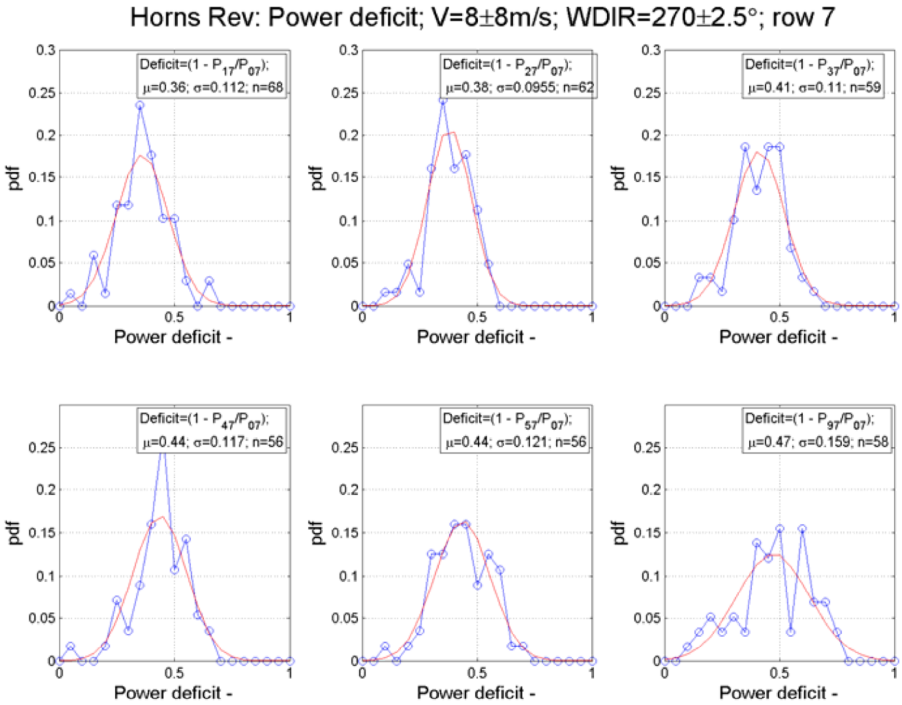

Figure 4: The probability distribution of the power deficit along the row 7.

RESULTS

This article focuses on three benchmark test cases analyzed in the EERA-DTOC and IEA-Task 31 WakeBench projects. The first one is the single wake power deficit test case, the second one is the power deficit along a row of wind turbines for different inflow wind direction bins and the third one is the maximum power deficit, between two turbines, at different downstream distance as a function of the inflow turbulence intensity.

Single wake power deficit test case

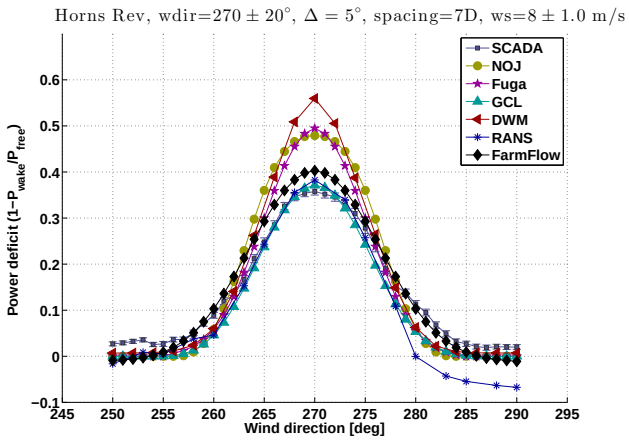

Figure 5: Single wake power deficit between pairs of wind turbines with a 5°averaging window.

The power deficit between wt17 and wt07 in the 270° wind direction, with an averaging window of 5° is illustrated in fig. 5. The wind direction is measured using the nacelle position of wt7 (NP07). The wind speed is measured using an inversed power curve using the power production of the first wind turbine in each row. When directly aligned in 270°, the wind turbines have a spacing of 7 rotor diameters.

GCL, RANS and FarmFlow seem to match the closest the SCADA wake deficit shape, while the other ones seem to over-predict the wake deficit. In the central part of the wake. The RANS model has an asymmetry on the right side that seems to indicate a speed up of the flow. This effect is not visible in the SCADA data.

Note that the SCADA point at 270° corresponds to the probability distribution data presented in top left fig. 4. This shows that even though the error bars are quite small (i.e the standard uncertainty is small), all the wake models are still within the SCADA measurement spreading.

Power deficit along a row of turbines

The power deficit between wt07 and the downstream turbines in row7 in the 270° wind direction, with an averaging window of $\Delta = 5°$, 15°, and 30° is illustrated in fig. 6, 7 and 8. The wind direction is measured using the nacelle position of wt07 (NP07). The wind speed is measured

using an inversed power curve using the power production of wt07. When directly aligned in 270°, the wind turbines have a spacing of 7 rotor diameters.

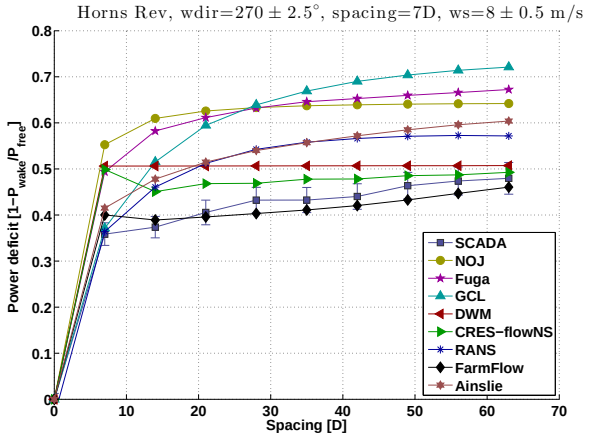

Figure 6: Power deficit along a row of turbine with and inflow wind direction bin of $\Delta = 5°$

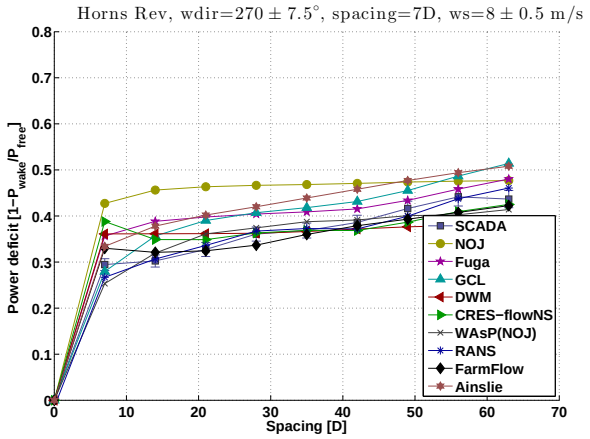

Figure 7: Power deficit along a row of turbine with and inflow wind direction bin of $\Delta = 15°$

As a general trend, most models seem to over-predict the wake deficit for small wind direction averaging window (Δ), and have a closer prediction to the largest Δ. Some of the models, like GCL and RANS have a close estimate of the first turbine downstream, and then seem to deviate gradually from the SCADA points for $\Delta = 5°$ (fig. 6). In the three Δs, FarmFlow seems to consistently match closely the shape of the SCADA points. Most models, except NOJ, WAsP/NOJ and DWM, seem to be very close to the SCADA point shape in $\Delta = 30°$ (fig. 8).

Note that the SCADA points with an averaging window of 5° fig. 6 corresponds to the

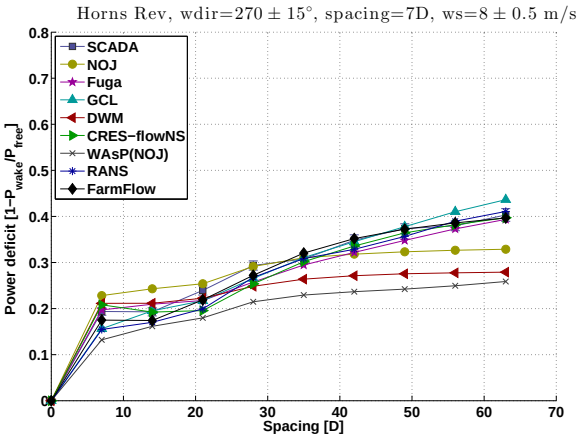

Figure 8: Power deficit along a row of turbine with and inflow wind direction bin of $\Delta = 30°$

probability distribution data plots in fig. 4. This shows that even though the error bars are quite small (i.e the standard uncertainty is small), all the wake models are still within the SCADA measurement spreading.

Maximum power deficit for different inflow turbulence intensity

The maximum power deficit between two turbines for different inflow turbulence intensity is illustrated at 7 rotor diameters (fig. 9) ad 10.4 rotor diameters (fig. 10).

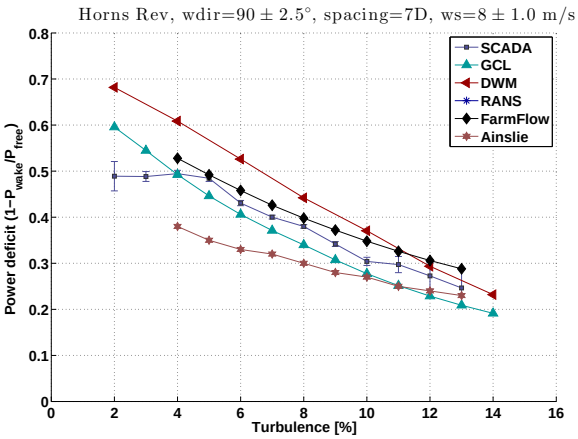

Figure 9: Maximum power deficit for different inflow turbulence intensity and a wind turbine spacing of 7 rotor diameters

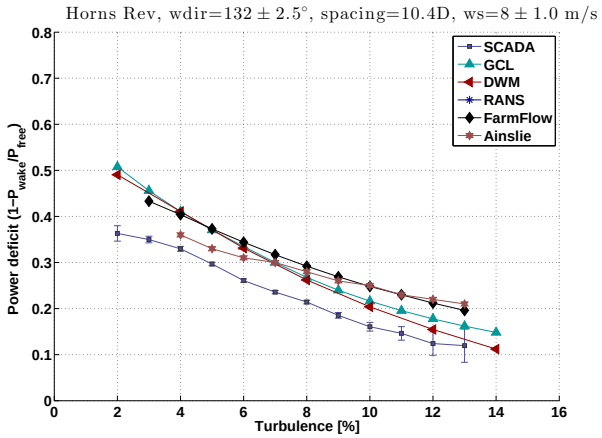

Figure 10: Maximum power deficit for different inflow turbulence intensity and a wind turbine spacing of 10.4 rotor diameters

Most models seem to capture the trend correctly.All the models have a tendency to over-predict the maximum wake deficit at 10.4D, even though some of the models (e.g. GCL and Ainslie) are under-predicting the wake deficit at 7D. There does not seem to be a model clearly better than the other ones in this benchmark.

DISCUSSION

As discussed in the data analysis section, the small wind direction sectors Δs are very sensitive to the wind direction uncertainty used to select the data. As the uncertainty in wind direction is still quite high because of the sensor used (the nacelle position sensor follows the yaw misalignment), the benchmarks based on the small Δs might not give a good representation of the accuracy of the wake models. The uncertainty in wind direction creates an artificially lower wake deficit during the ensemble averaging. In these smaller Δs the models seem in majority to over-predict the wake deficit, which might be because the SCADA is heavily influenced by the wind direction uncertainty. When looking at the probability distribution of the SCADA measurements, most of the models do seem to remain within the spreading of the data. With this in mind, it is quite difficult to pick one model performing better than the other one over the test castes $\Delta = 5^\circ$ and $\Delta = 15^\circ$.

For modeling more fairly the small Δs, it could be necessary to post-process the wake models to account for the effect of wind direction uncertainty in the measurement averaging as proposed by Gaumond et al. [4].

The wind direction sector $\Delta = 30^\circ$ is the Δ normally used for calculating the AEP. As estimating accurately the AEP is the main focus of the current EERA-DTOC project, it should be

here considered that $\Delta = 30^\circ$ is the more important benchmark compared with the two others Δs benchmarks. So even thought most models seem to over-estimate the wake deficit in the smaller Δs, many are still performing quite well in $\Delta = 30^\circ$ and could therefore still produce very accurate AEPs.

The results of fig. 6, 7 and 8 are very close to a previously published work on the same Horns Rev wind farm case in the UpWind project [18]. While since then the SCADA data have been refined (i.e the measurements points have a lower uncertainty), and some of the models have been re-factored for offshore conditions, the main conclusions stay the same. The wake model still over predict the narrow sectors, probably due to the wind direction uncertainty, while they perform satisfyingly for the larger sector.

Looking at the benchmark results, the wake accumulation method might have a strong influence the shape of the wake deficit along a row of turbine. The DWM (i.e. using the maximum) and NOJ flavors (i.e. using a RSS) seem to perform the least well to match the SCADA shape, even at large Δs. They both present flatter trends compared with the SCADA measurements, that seems to indicate that if the wind farm was larger their results would deviate even more strongly. This results are in agreement with previous studies [4,6].

It is somewhat difficult to judge the importance of the other sub-model assumptions as most models use quite different combinations. For instance, it is not clear how sensible the models are regarding the number of points needed to produce the hub wind speed. For answering this specific question, it would be more appropriate to carry out a sensitivity analysis on each specific model.

Similarly, only one model uses an advanced aero-elastic model with a controller for the wind turbine (DWM). It is not clear from the results that this would be giving a more realistic estimate of the wind farm annual energy production. Here again it would be interesting to test each model independently if they would benefit from a more sophisticated wind turbine model.

While they seem to perform satisfyingly in the first two test cases, the more computationally intensive non-linear CFD models such as RANS and CRESflowNS do not seem to show any more realistic behavior compared with the order of magnitude faster CFD models such as FarmFlow, FUGA or even the engineering models such as Ainslie or GCL.

CONCLUSIONS AND FUTURE WORK

This article presented the results of a benchmark campaign carried on within the EERA-DTOC project, in collaboration with the IEA-Task 31 ”WakeBench” project. A wide scope of different wake models have been compared on different types of test cases. Because of the complexity of dealing with large offshore wind farm SCADA data, it is very challenging to create comparable results to the wind farm wake models. Especially, the issue of wind direction uncertainty is found to create an artificially lower wake deficit. As the models are not directly taking into account this uncertainty it is important to take a step back from the benchmarking results and being pragmatic about the performance of the different models. For instance, the performance of

the wake models in small wind direction averaging windows are not so critical when estimating the annual energy production, which is the focus of EERA-DTOC.

Within the EERA-DTOC project another test case is planned on the Horns Rev benchmark. The wind farm efficiency polar distribution, should give a more quantifiable metric of the accuracy of the wind farm wake models to estimate AEPs. Another benchmark is also planned on the Lillgrund wind farm in collaboration with the IEA-Task 31 "WakeBench" and Vattenfall AB, the wind farm owner. The wind turbines are larger and more closely spaced, which should challenge the wake models in a different manner than the Horns Rev wind farm did.

ACKNOWLEDGEMENTS

This work is supported by the EU EERA-DTOC project nr. FP7-ENERGY-2011/n 282797, and of the Danish EUDP-WakeBench project nr. 64011-0308. The Horns Rev data was gratefully provided through previous projects by the wind farm owners Vattenfall AB and DONG Energy AS.

REFERENCES

[1] Hansen K., Barthelmie R.J., Jensen L., Sommer A., 2011a, The impact of turbulence intensity and atmospheric stability on power deficits due to wind turbine wakes at Horns Rev wind farm, Wind Energy, doi: 10.1002/we.512, 2001.
[2] Hansen K., et al., 2011b, Guideline to wind farm wake analysis. In UPWIND 1A2 Metrology, Final Report, Chapter 8, ECN-E–11-013, February 2011.
[3] Hansen K., et al., 2011c, Classification of atmospheric stability for offshore wind farms. In UPWIND 1A2 Metrology, Final Report, Chapter 10, ECN-E–11-013, February 2011.
[4] Gaumond M., et al., 2011c, Evaluation of the wind direction uncertainty and its impact on wake modelling at the Horns Rev offshore wind farm, Wind Energy, 2013.
[5] Anderson M., Simplified soultion to the eddy viscosity wake model, www.res-americas.com, 2009.
[6] Habenicht G. Offshore wake modelling, Presentation at Renewable UK Offshore Wind, www.res-group.com, 2011.
[7] Larsen T.J., Hansen A.M., How 2 HAWC2, the user's manual. Technical Report, Risø-R-1597, DTU-Wind Energy, Risø, Denmark 2007.
[8] Ainslie J.F., Calculating the flow field in the wake of wind turbines, Journal of Wind Engineering and Industrial Aerodynamics, 27: p 213-224, 1988.
[9] Crespo, A., Hernández, J., Fraga, E., Andreu, C., Experimental validation of the UPM computer code to calculate wind turbine wakes and comparison with other models. Journal of Wind

Engineering, 27, p 77–88, 1998.
[10] Mortensen N.G., Heathfield D.N., Rathmann O., Nielsen M., Wind Atlas Analysis and Application Program: WAsP 10 Help Facility. Technical report, Risø National Laboratory, Roskilde, Denmark, December 2011.
[11] N.O. Jensen. A note on wind generator interaction. Technical Report Risø-M- 2411, Risø National Laboratory, Roskilde, Denmark, 1983.
[12] Ott S., Berg J., Nielsen M., "Linearised CFD Models for Wakes". Technical Univ. of Denmark, Risoe National Lab. for Sustainable Energy. Wind Energy Div. Risoe-R-1772(EN) ISBN 978-87-550-3892-9. Available online.
[13] Prospathopoulos, J. M. and Chaviaropoulos, P.K., "Numerical simulation of offshore wind farm clusters", European Wind Energy Association, Conference proceedings 2013.
[14] Chaviaropoulos P. K. and Douvikas D. I., "Mean-flow-field Simulations over Complex Terrain Using a 3D Reynolds Averaged NavierStokes Solver," Proceedings of ECCOMAS 98, Vol. I, Part II, pp. 842-848. 1998.
[15] Larsen GC. A simple stationary semi-analytical wake model. Technical Report, Risø-R-1713(EN) August, Risø DTU 2009.
[16] Larsen GC, Madsen HA, Thomsen K, Larsen TJ. Wake meandering: a pragmatic approach. Wind Energy Jul 2008; 11(4):377–395, doi:10.1002/we.267.
[17] Madsen HA, Larsen GC, Larsen TJ, Troldborg N, Mikkelsen R. Calibration and Validation of the Dynamic Wake Meandering Model for Implementation in an Aeroelastic Code. Journal of Solar Energy Engineering 2010; 132(4):041 014, doi:10.1115/1.4002555.
[18] Barthelmie R.J., Hansen K., Frandsen S.T., Rathmann O., Schepers J.G., Schlez W., Phillips J., Rados K., Zervos A., Politis E.S., Chaviaropoulos P.K., Modelling and Measuring Flow and Wind Turbine Wakes in Large Wind Farms Offshore. Wind Energy, doi:10.1002/we.348, 2009.
[19] Barthelmie R.J., Barthelmie, Larsen G.C., Pryor S., Jørgensen H.E., Bergström H., Schlez W., Rados K., Lange B., Vølund P., Neckelmann S., Mogensen S., Schepers G., Hegberg T., Folkerts L., Magnusson M., ENDOW (efficient development of offshore wind farms): modelling wake and boundary layer interactions. Wind Energy. 2004. DOI: 10.1002/we.121.
[20] Réthoré P.-E., Wind Turbine Wake in Atmospheric Turbulence, PhD Thesis, Aalborg University, 2009.
[21] Rathmann O, Ott S & Kelly MC , 'Wind farm wake effects estimations by a mosaic tile wake model'. in: Proceedings. EWEA 2011.